



Original article

Myocardial dysfunction identified by three-dimensional speckle tracking echocardiography in type 2 diabetes patients relates to complications of microangiopathy



Mami Enomoto (MD)^a, Tomoko Ishizu (MD, PhD, FJCC)^{a,b,*}, Yoshihiro Seo (MD, PhD, FJCC)^a, Yuri Kameda (BSc)^c, Hiroaki Suzuki (MD, PhD)^d, Hiroshi Shimano (MD, PhD)^d, Yasushi Kawakami (MD, PhD)^{a,b}, Kazutaka Aonuma (MD, PhD, FJCC)^a

^a Cardiovascular Division, Faculty of Medicine, University of Tsukuba, Tsukuba, Japan

^b Department of Clinical Laboratory Medicine, Faculty of Medicine, University of Tsukuba, Tsukuba, Japan

^c Department of Medical Sciences, University of Tsukuba, Tsukuba, Japan

^d Division of Endocrinology and Metabolism, Faculty of Medicine, University of Tsukuba, Tsukuba, Japan

ARTICLE INFO

Article history:

Received 4 November 2015
Received in revised form 9 March 2016
Accepted 15 March 2016
Available online 14 April 2016

Keywords:

Diabetic cardiomyopathy
Three-dimensional echocardiography
Myocardial strain

ABSTRACT

Background: The clinical effect of diabetic microangiopathy on left ventricular (LV) function is still uncertain. The purpose of this study was to assess the relation between diabetic microvascular complications and comprehensive myocardial deformation measurements using three-dimensional (3D) speckle tracking echocardiography.

Methods: Seventy-seven asymptomatic patients with type 2 diabetes mellitus (DM) and 35 age-matched healthy control subjects underwent 3D echocardiography. Patients with coronary artery disease or LV ejection fraction <50% were excluded. Presence of proliferative retinopathy, microalbuminuria as nephropathy, and decreased coefficient of variation of R-R intervals (CVRR) <3% as cardiac autonomic neuropathy were defined as diabetic microvascular complications.

Results: LV ejection fraction, LV mass index, and global radial strain did not differ between control and DM patients. However, global longitudinal and circumferential strain and endocardial area change ratio were lower in patients with DM than in the controls ($-12.0 \pm 3.0\%$ vs. $-16.2 \pm 1.9\%$, $-27.7 \pm 7.1\%$ vs. $32.2 \pm 5.7\%$, $-37.6 \pm 7.6\%$ vs. $44.0 \pm 6.2\%$, respectively, $p < 0.001$). In DM patients, longitudinal strain is related to CVRR ($R = 0.58$, $p < 0.001$), retinopathy stage, and nephropathy stage.

Conclusions: Diabetic microangiopathy and its accumulated effects significantly related to subclinical LV dysfunction are characterized by impaired longitudinal shortening.

© 2016 Japanese College of Cardiology. Published by Elsevier Ltd. All rights reserved.

Introduction

Diabetic cardiomyopathy, defined as left ventricular (LV) dysfunction occurring independently of coronary artery disease and hypertension [1], might be an important substrate for developing heart failure [2]. Although diabetic cardiomyopathy is thought to be a multifactorial disease, the pathophysiological significance of microvascular complications remains unclear [3]. Among the diabetic microangiopathies [4], cardiac autonomic

neuropathy [5,6] is focused on because it has been reported to relate to adverse clinical outcomes [7] and is commonly observed in many diseases such as symptomatic heart failure, chronic kidney disease, myocardial infarction, hibernating myocardium, and in cardiac transplantation [8]. Furthermore, retinopathy [9,10] and nephropathy [11] show an apparent effect on the occurrence of heart failure and its outcome.

Two-dimensional (2D) speckle tracking echocardiography (STE) has revealed systolic, and not just diastolic [12], longitudinal dysfunction to be a sign of early mechanical damage in the diabetic heart [13] and poor prognosis [14]. Three-dimensional (3D) STE has been introduced as a promising quantitative technique allowing a more accurate and comprehensive evaluation of myocardial deformation than conventional cardiovascular imaging techniques of LV deformation [15]. Compared to 2D echocardiography, the 3D

* Corresponding author at: Department of Clinical Laboratory Medicine, Faculty of Medicine, University of Tsukuba, 1-1-1 Tennodai, Tsukuba, Ibaraki 305-8575, Japan. Tel.: +81 29 853 3142; fax: +81 29 853 3143.

E-mail address: tomoco@md.tsukuba.ac.jp (T. Ishizu).

approach is not affected by cut-down views and performs tracking over time in all three dimensions, avoiding any potential out-of-plane motion of the ultrasonic speckles [16]. Accordingly, the aim of the present study was to reveal a complete picture of LV systolic deformation abnormality in asymptomatic patients with diabetes mellitus (DM) using 3D-STE comprehensively and to investigate the effect of the degree of DM microvascular disease on subclinical LV dysfunction.

Methods

Study population

We enrolled 77 hospitalized patients with type 2 DM requiring diabetes education in this study. Patients with coronary artery disease or LV ejection fraction (LVEF) <50%, other than sinus rhythm, significant valvular disease, and inadequate echocardiographic image quality for analysis were excluded. Patients with coronary artery disease were excluded by coronary computed tomography angiography or myocardial scintigraphy. Reasons for performing computed tomography or scintigraphy included carotid atherosclerosis, ischemic changes on electrocardiogram (ECG), positive exercise ECG test results, or LV wall motion abnormalities on echocardiography. ECG abnormalities, such as Q waves, ST-T changes, and negative T waves, positive exercise ECG test results, and LV wall motion abnormalities on echocardiography were considered to be suggestive of the presence of coronary artery disease. The control population consisted of 35 age-matched healthy subjects. Ethical approval was obtained from the local institutional review committee, and all patients provided written informed consent.

Echocardiographic examinations

Echocardiographic examinations were performed with an Aplio-Artida™ (Toshiba Medical Systems Co., Tochigi, Japan) echocardiographic system with a multi-frequency transducer. LV diameters were measured on a 2D-guided M-mode image. The LV mass index was calculated from 2D echocardiographic measurements using the area-length formula at end-diastole and corrected for body surface area. LV volumes and LVEF were measured by biplane Simpson's method in apical 4- and 2-chamber views. The peak velocities of early (E) and late (A) mitral inflow, the ratio E to A (E/A), and the deceleration time of the E-wave were measured using pulsed Doppler echocardiography with the sample volume at the tip of the mitral valve leaflet. Using tissue Doppler imaging, the peak early diastolic velocities of (E') at the basal septal and lateral mitral annulus were obtained in the apical 4-chamber view.

3D-STE

Full-volume ECG-gated 3D data sets were acquired from apical positions using a matrix array transducer (3 V). To obtain these data sets, 6 sectors were scanned and automatically integrated into a wide-angle (70 × 70 degrees) pyramidal data image covering the entire LV. The volume rate of each image was set at approximately 30 Hz. The data were stored and transferred to a computer (Inspiron 1300; Dell Inc., Round Rock, TX, USA) for off-line analysis. The images were analyzed for wall deformation with specialized software (3D Wall Motion Tracking, Toshiba Medical Systems Co.). First, the endocardial border of the 4-chamber image at end-diastole was traced manually, followed by manual tracing of the epicardial border. Then, the same tracing processes were repeated in the 2-chamber image. After these long-axis tracings were complete, 3D myocardial surfaces were automatically reconstructed, and fine

adjustments were made to the traced borders on the short-axis images.

We identified the tracking quality by eye-ball based on both endo- and epicardial trace lines on multiplanar reconstruction images. Finally, 6 LV basal, 6 mid, and 4 apical segment measurements (total 16) of strain were calculated as $\text{strain} = [L(t) - L_0]/L_0$, where $L(t)$ is the segment length at time t and L_0 is the segment length at the end diastole. Then, the following parameters were obtained: global radial strain (GRS), global circumferential strain (GCS), global longitudinal strain (GLS), and area change ratio (ACR). GRS was measured based on both endo- and epicardial tracking, and GLS, GCS, and ACR were calculated based on endocardial surface deformation.

Reproducibility of 3D-STE

We selected 10 studies at random for assessment of intra- and interobserver reproducibility of speckle tracking analysis. To test intra-observer variability, a single observer analyzed the data twice. The second analysis was done 1 week after the first analysis. To test interobserver variability, a second observer analyzed the data without knowledge of the first observer's measurements. Reproducibility was assessed as the mean percent error (absolute difference divided by the mean of the two individual observations).

Complications of diabetes

We evaluated cardiac autonomic nervous system function by use of the coefficient of variation of R-R intervals (CVRR). Analysis of beat-to-beat fluctuations in heart rate provides a sensitive, quantitative, and noninvasive measure of the functioning of the principal rapidly reacting cardiovascular control systems: the sympathetic and parasympathetic nervous systems [17]. CVRR measurements were obtained based on previously reported methods [18]. First, the patients were kept at rest in a supine position for 15 min prior to monitoring by ECG. The R-R intervals were measured for 3 min on the ECG. The CVRR was obtained from the recorded R-R intervals by dividing their standard deviation (SD) by the mean. The normal value of CVRR of 40- to 50-year-old subjects is $3 \pm 1\%$. Therefore, an abnormal CVRR was defined as $<3\%$ in the present study.

The stage of diabetic retinopathy was diagnosed by ophthalmologists based on a modification of the Davis classification: simple retinopathy as class A and proliferative retinopathy as class B. The nephropathy stage was diagnosed according to the presence of urine albumin and estimated glomerular filtration rate (eGFR). Stage 1 was defined as no albuminuria and normal/high eGFR, stage 2 as microalbuminuria and normal/high eGFR, stage 3 as persistent proteinuria and decreased eGFR, stage 4 as persistent proteinuria and extremely decreased GFR, and stage 5 as patients receiving hemodialysis. Microangiopathy total burden was calculated as the sum of the following scores: CVRRs of the upper, middle, and highest tertile were scored as 0, 1, and 2, respectively; class A retinopathy was scored as 1 and class B as 2; and nephropathy stage 1 was scored as 1, and \geq stage 2 was scored as 2.

Statistical methods

All values are expressed as mean \pm SD. The χ^2 -test was used for categorical variables. Comparisons between two groups were performed using the Student t -test for continuous variables. Analysis of variance (ANOVA) was used to compare results among groups divided by the degree of microvascular complication, and post hoc analysis was performed using Scheffé's test. Scheffé's partial correlations for confounding variables were performed to evaluate the association among the nephropathy stage, retinopathy stage, and LV 3D-STE data. The data were analyzed using standard statistical

software (SPSS ver. 18.0, SPSS Inc., Chicago, IL, USA). A *p*-value of <0.05 was considered to be statistically significant.

Results

In comparisons between control subjects and patients with DM, no significant differences existed in age, sex, body mass index, blood pressure, or heart rate (Table 1). The patients with DM showed a high fasting glucose level, very high hemoglobin A1c level, normal range of mean N-terminal pro B-type natriuretic peptide (NT-proBNP) levels, and normal serum lipid profiles. Insulin was prescribed for 35 (45%) patients.

Microvascular complications of DM

In patients with DM, the mean CVRR was $2.8 \pm 1.2\%$. Retinopathy class was identified as no retinopathy in 50 patients, class A in 15 patients, and class B in 12 patients. Nephropathy stage was identified as class 1 in 58 patients, class 2 in 10 patients, and class 3 in 9 patients (Table 2).

Echocardiographic parameters

Conventional echocardiography showed significantly lower *E'* in the DM group compared with that in the control group. There were no significant differences in LVEF, LV chamber size and thickness, left atrial size, and transmitral flow velocity profiles (Table 3).

3D-STE measurements

The respective intra- and interobserver variabilities were as follows: 17% and 20% for GRS, 9% and 14% for GCS, 8% and 10% for GLS, and 4% and 10% for ACR. 3D-STE measurements are shown in Fig. 1. GLS, GCS, and the ACR in the patients with DM were smaller than those in the control subjects. GRS showed no significant difference between the DM and control groups.

Table 1
Baseline patient characteristics and diabetes treatments.

	Healthy controls (<i>n</i> = 35)	DM (<i>n</i> = 77)	<i>p</i> value
Age (years)	52 ± 16	56 ± 15	0.70
Sex (men/women)	18/17	53/24	0.07
Body mass index	22.1 ± 2.2	23.2 ± 3.5	0.13
Systolic blood pressure (mmHg)	122.9 ± 17.2	119.8 ± 21.4	0.55
Diastolic blood pressure (mmHg)	73.2 ± 13.4	70.3 ± 13.6	0.39
Heart rate (beats/min)	65.5 ± 12.7	66.1 ± 11.9	0.88
Hypertension coexisting, <i>n</i> (%)		35 (45)	
Laboratory tests			
Hemoglobin A1c (%)		10.6 ± 2.5	
Fasting blood glucose (mg/dl)		162 ± 49	
Fasting serum insulin (μg/dl)		6.7 ± 6.4	
Triglyceride (mg/dl)		146 ± 64	
HDL cholesterol (mg/dl)		44 ± 13	
LDL cholesterol (mg/dl)		119 ± 36	
NT-proBNP (pg/mL)		55 ± 73	
Microvascular complications			
Neuropathy complication, <i>n</i> (%)		48 (62)	
Retinopathy complication, <i>n</i> (%)		27 (35)	
Nephropathy complication, <i>n</i> (%)		64 (83)	
DM medication			
Insulin, <i>n</i>		35	
Oral drug, <i>n</i>		33	
Insulin + oral drug, <i>n</i>		6	
Diet treatment, <i>n</i>		3	

NT-proBNP, N-terminal pro-B-type natriuretic peptide; DM, diabetes mellitus; HDL, high-density lipoprotein; LDL, low-density lipoprotein.

Table 2
Parameters related to complications of diabetes.

	DM (<i>n</i> = 77)
CVRR (%)	2.78 ± 1.24
Class of retinopathy (no/A/B)	50/15/12
Class of nephropathy (1/2/3)	58/10/9

CVRR, coefficient of variation of R-R intervals; DM, diabetes mellitus.

Relations between 3D-STE parameters and patient characteristics and conventional echo parameters

As shown in Table 4, body mass index and hemoglobin A1c showed no relation with strain parameters. GLS significantly related to elevated LV mass but not to systolic or diastolic blood pressure or any of the laboratory test values including NT-proBNP level. Except for GRS, all 3D-STE parameters related to LVEF.

Relations between 3D-STE parameters and microvascular complications

Among the 3D-STE parameters, GLS was significantly related to CVRR, retinopathy stage, and nephropathy stages (Fig. 2). GLS was significantly impaired in patients with a microangiopathy total score >1 compared with that in the patients without microangiopathy (Fig. 3). Furthermore, patients with a score of 6, indicative of severe microangiopathy, had a lower GLS than patients with a score of 1 or 0. The other 3D-STE parameters of GCS, GRS, and ACR showed no significant relation to the status of DM complications.

Relations between 3D-STE parameters and hypertension

In the 77 patients with DM, 35 (45%) patients were complicated with hypertension (DM-HT) and 42 (55%) patients had a normal blood pressure (DM-normo-BP). Systolic blood pressure was significantly higher, and GRS was significantly impaired in the DM-HT group compared with the DM-normo-BP group, whereas there were no significant differences in GCS and GLS between the two groups. Angiotensin II receptor blockers (ARB) were prescribed for 16 (46%) patients and a calcium channel blocker (CCB) was prescribed for 13 (37%) patients in the DM-HT group.

Systolic blood pressure showed no significant difference between the patients with and without ARB or CCB, but GRS was significantly impaired in the patients without ARB compared with that in those with ARB. GCS was also significantly impaired in the patients without a CCB compared with that in those with a CCB.

Table 3
Echocardiographic variables.

Variable	Control (<i>n</i> = 35)	DM (<i>n</i> = 77)	<i>p</i> value
LV ejection fraction (%)	68.9 ± 5.6	66.3 ± 7.7	0.82
LV end-diastolic dimension (mm)	46.7 ± 4.2	45.9 ± 5.2	0.41
LV end-systolic dimension (mm)	27.4 ± 3.4	29.0 ± 4.7	0.11
Septal wall thickness (mm)	8.2 ± 1.1	8.7 ± 1.8	0.22
LV posterior wall thickness (mm)	8.5 ± 1.04	8.7 ± 1.3	0.38
LV mass index (g/m ²)	90.5 ± 17.4	90.1 ± 29.2	0.94
LAVI (mL/m ²)	26.2 ± 9.2	26.2 ± 8.7	0.98
<i>E'</i> (cm/s)	13.0 ± 2.4	9.7 ± 3.2	0.004
Mitral E/A	1.3 ± 0.5	1.1 ± 0.5	0.11
DcT (ms)	203.5 ± 44.7	228 ± 63.8	0.07
<i>E'/E'</i>	6.7 ± 1.5	8.2 ± 3.0	0.06

DcT, deceleration time of E-wave; DM, diabetes mellitus; *E'*, early diastolic mitral annular velocity; LAVI, left atrial volume index; LV, left ventricular.

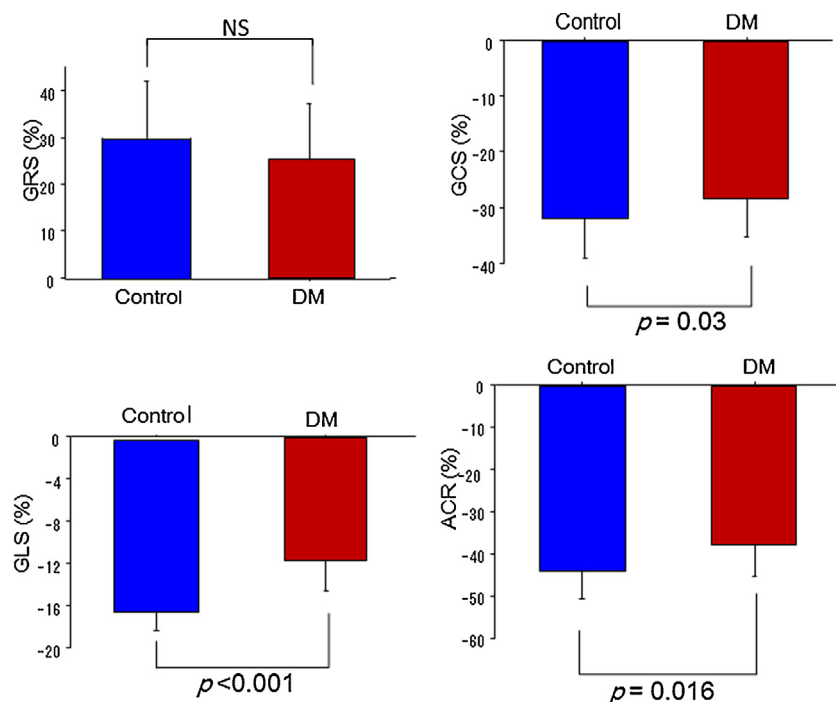


Fig. 1. Left ventricular 3-dimensional speckle tracking measurements in patients with diabetes and control subjects. Although GRS (upper, left) was similar in both groups, the DM group showed significantly impaired GCS (upper right), GLS (lower left), ACS (lower right), compared to the control group. ACR, area change ratio; DM, diabetes mellitus; GCS, global circumferential strain; GLS, global longitudinal strain; GRS, global radial strain.

Discussion

This 3D-STE study resulted in two major findings. First, 3D-STE-derived measures of GLS, GCS, and ACR were impaired, and LVEF was preserved in patients with type 2 DM. Second, GLS was related with both the presence and the accumulation of diabetic microvascular complications and especially with cardiac autonomic neuropathy.

Longitudinal systolic dysfunction in the diabetic heart

Longitudinal strain impairment in DM patients has also been demonstrated previously using multiple imaging modalities such as cardiac magnetic resonance imaging [13,19], tissue Doppler imaging [20], and 2D-STE [21,22] or 3D-STE [23]. Therefore, it is generally agreed that LV longitudinal dysfunction appears to be an early manifestation of diabetic cardiomyopathy. The underlying

mechanism of the longitudinal dysfunction has been proposed to be due to subendocardial damage [24].

Circumferential, radial, and area strain in the diabetic heart

In contrast to the consistent impairment in longitudinal strain, circumferential strain and radial strain abnormalities vary depending on the study population. In the present study, circumferential strain impairment depended on patient age in the DM group, although the control group showed no significant relation between GCS and age ($p = 0.67$). Circumferential strain has been reported to relate to the function of the midwall circumferential fiber layer [25]. Thus, age-dependent circumferential dysfunction suggests disease progression to the midwall from the endocardium.

Radial strain in the DM group was not significantly different from that in the control group; however, in the DM group, radial

Table 4

Correlates of 3D-STE parameters and background characteristics and standard echo parameters.

Variable	GLS		GCS		GRS		ACR	
	R	p	R	p	R	p	R	p
Age		0.81	-0.26	0.02		0.11		0.09
BMI		0.95		0.59		0.70		0.53
SBP		0.65		0.48	-0.35	0.003		0.31
DBP		0.12		0.06	-0.27	0.022		0.06
HbA1c		0.30		0.24		0.95		0.30
DM duration		0.89		0.14		0.45		0.24
LVEF	-0.24	0.04	-0.30	0.01		0.12	-0.33	0.005
LV mass	0.23	0.04		0.43	-0.27	0.027		0.31
LAVI		0.87		0.30		0.32		0.31
E/A		0.08		0.26		0.19		0.63
E'		0.05		0.49	0.27	0.021		0.84

ACR, area change ratio; BMI, body mass index; DBP, diastolic blood pressure; DM, diabetes mellitus; GCS, global circumferential strain; GLS, global longitudinal strain; GRS, global radial strain; HbA1c, hemoglobin A1c; LAVI, left atrial volume index; LV, left ventricular; LVEF, LV ejection fraction; SBP, systolic blood pressure; STE, speckle tracking echocardiography.

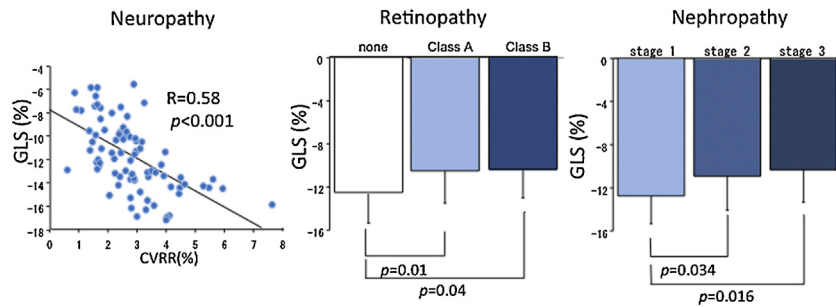


Fig. 2. Comparison between global longitudinal strain and diabetic microangiopathy status in the DM group. Scatter plot with regression line (left) indicates significant negative relation between GLS and CVRR of neuropathy. Impairment of GLS was related with presence or absence, but not severity, of retinopathy (middle) and nephropathy (right). CVRR, coefficient of variation in R-R interval; DM, diabetes mellitus; GLS, global longitudinal strain.

strain is related with blood pressure, LV hypertrophy, and E' . Previous reports demonstrating radial strain impairments in DM patients [21,22] also showed significantly greater blood pressure, E/E' , and left atrial volume compared with those in the control subjects. In contrast, the present study showed similar blood pressure and LV mass and E/E' values between the DM group and control subjects. Although our study patients showed milder diastolic dysfunction than that in previous studies, these facts may imply that the results of both previous studies and our study showed the consistent feature that radial strain reflects high blood pressure, LV hypertrophy, and diastolic dysfunction in the diabetic heart.

Cardiac autonomic neuropathy and subclinical LV dysfunction

Cardiac autonomic neuropathy, represented by an abnormal CVRR, is one of the significant variables related to GLS in the present study. It was previously reported that cardiac autonomic neuropathy is associated with LV filling abnormality [26], tissue Doppler-derived diastolic function [27], myocardial fibrosis, and coronary flow reserve impairment [28,29]. Recently, Mochizuki et al. [30] reported that 2D-STE-derived LV GLS in asymptomatic DM patients with diabetic neuropathy and preserved LVEF is significantly impaired compared to that in patients without diabetic neuropathy in spite of similar conventional echocardiographic parameters. The results of the present study are consistent with their findings and support the concept that diabetic cardiac autonomic neuropathy is cross-related to LV systolic longitudinal dysfunction in a quantitative manner. Because cardiac autonomic neuropathy is a related adverse outcome, the early noninvasive detection of subclinical cardiomyopathy in cardiac autonomic

neuropathy is important. Longitudinal dysfunction could be a candidate for the detection of cardiac autonomic neuropathy relating to cardiac dysfunction in DM patients. Although investigation of the pathophysiological mechanism is beyond the scope of this study, a possible explanation for cardiac autonomic neuropathy causing augmentation of longitudinal dysfunction might be as follows: (1) CVRR is the marker of parasympathetic denervation of the heart [17], (2) parasympathetic denervation should cause a relative increase in sympathetic tone, (3) sympathetic hypertonia generates oxidative stress, (4) oxidative stress induces tissue inflammation, (5) inflammation is followed by perivascular and then interstitial myocardial fibrosis, and (6) fibrosis, if it predominantly occurs in the subendocardial layer, results in longitudinal systolic dysfunction [24].

Study limitations

This study has several limitations. First, assessment of cardiac autonomic neuropathy is of an indirect nature, and no data were obtained from metaiodobenzylguanidine scintigraphy. Because we included asymptomatic patients, invasive examinations that include radiation might not be acceptable for all subjects included in the study. Second, GRS did not change significantly despite the significant decrease in GLS and GCS in the patients with DM. If the myocardial volume is constant throughout the cardiac cycle, GRS should be the product of GLS times GCS. We believe that the non-significant results of GRS in this setting might be due to the suboptimal tracking of the speckle signal of subendocardial tissue in 3D echocardiography. According to the suboptimal reproducibility of GRS when the CVRR is over 10%, we think that caution is imperative in the assessment of the results of GRS by 3D-STE.

Another limitation is that a comparison of 3D- with 2D-STE was not performed. 2D-derived GLS is an adequately proven marker for subclinical myocardial dysfunction, and 3D-derived GLS showed consistent results with 2D-derived GLS regarding the linear correlation between diabetic neuropathy and systolic longitudinal dysfunction. These facts suggest the equivalent utility of both 2D- and 3D-derived GLS in assessing subclinical systolic function in diabetic patients.

Finally, this is a cross-sectional study, and we lack follow-up data on the patients. Prospective studies comparing direct cardiac sympathetic denervation with 3D-STE measurements are required in the future, and they should reveal whether GLS is related to the morbidity and mortality of diabetic heart failure. Furthermore, it is mandatory for us to evaluate the effects of drug therapy for diabetes and assess the LV deformation response in a future prospective study.

Clinical implications

Heart failure is one of the major causes of mortality in diabetic patients [2]. In addition, DM is a major risk factor for developing

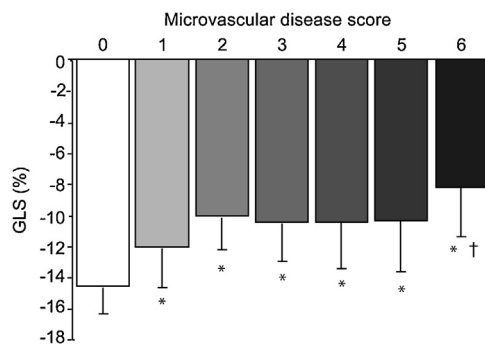


Fig. 3. Global longitudinal strain and microangiopathy burden score. Microangiopathy total burden was calculated as the sum of the following scores: CVRRs of the upper, middle, and highest tertile were scored as 0, 1, and 2, respectively; class A retinopathy was scored as 1 and class B as 2; and nephropathy stage 1 was scored as 1, and \geq stage 2 was scored as 2. CVRR, coefficient of variation in R-R interval; GLS, global longitudinal strain. * and †, $p < 0.005$ vs. microvascular disease score 0.

heart failure, especially in patients with preserved EF. Once heart failure progresses to the decompensated stage, no therapy can completely reverse cardiac remodeling or improve patient mortality. Therefore, early discrimination of patients at risk of myocardial damage during the early stage is crucial to prevent the development of manifest heart failure [3,31]. Because the results of the present study showed that microvascular damage is of key significance in subclinical LV endocardial impairment, patients with accumulated microvascular complications with impaired GLS could be targets for effective therapy along with watchful observation of disease progress.

Conclusion

3D-STE-derived longitudinal systolic dysfunction was associated with diabetic microvascular complications, and especially with cardiac autonomic neuropathy as assessed by CVRR, in asymptomatic non-ischemic patients with poorly controlled type 2 DM.

Funding sources

None.

Disclosures

None.

References

- [1] Boudina S, Abel ED. Diabetic cardiomyopathy revisited. *Circulation* 2007;115:3213–3223.
- [2] Cubbon RM, Adams B, Rajwani A, Mercer BN, Patel PA, Gherardi G, Gale CP, Batin PD, Ajjan R, Kearney L, Wheatcroft SB, Sapsford RJ, Witte KK, Kearney MT. Diabetes mellitus is associated with adverse prognosis in chronic heart failure of ischaemic and non-ischaemic aetiology. *Diab Vasc Dis Res* 2013;10:330–6.
- [3] Bando YK, Murohara T. Diabetes-related heart failure. *Circ J* 2014;78:576–83.
- [4] Shigeta T, Aoyama M, Bando YK, Monji A, Mitsui T, Takatsu M, Cheng XW, Okumura T, Hirashiki A, Nagata K, Murohara T. Dipeptidyl peptidase-4 modulates left ventricular dysfunction in chronic heart failure via angiogenesis-dependent and -independent actions. *Circulation* 2012;126:1838–51.
- [5] Ziegler D, Zentgraf CP, Perz S, Rathmann W, Haastert B, Doring A, Meisinger C. Prediction of mortality using measures of cardiac autonomic dysfunction in the diabetic and nondiabetic population: the MONICA/KORA Augsburg Cohort Study. *Diabetes Care* 2008;31:556–61.
- [6] Pop-Busui R, Evans GW, Gerstein HC, Fonseca V, Fleg JL, Hoogwerf BJ, Genuth S, Grimm RH, Corson MA, Prineas R. Action to Control Cardiovascular Risk in Diabetes Study Group. Effects of cardiac autonomic dysfunction on mortality risk in the Action to Control Cardiovascular Risk in Diabetes (ACCORD) trial. *Diabetes Care* 2010;33:1578–84.
- [7] Vinik AI, Ziegler D. Diabetic cardiovascular autonomic neuropathy. *Circulation* 2007;115:387–97.
- [8] Ji SY, Travin MI. Radionuclide imaging of cardiac autonomic innervation. *J Nucl Cardiol* 2010;17:655–66.
- [9] Wong TY, Rosamond W, Chang PP, Couper DJ, Sharrett AR, Hubbard LD, Folsom AR, Klein R. Retinopathy and risk of congestive heart failure. *JAMA* 2005;293:63–9.
- [10] Cheung N, Wang JJ, Rogers SL, Brancati F, Klein R, Sharrett AR, Wong TY, ARIC (Atherosclerosis Risk In Communities) Study Investigators. Diabetic retinopathy and risk of heart failure. *J Am Coll Cardiol* 2008;51:1573–8.
- [11] Gilbert RE, Connelly K, Kelly DJ, Pollock CA, Krum H. Heart failure and nephropathy: catastrophic and interrelated complications of diabetes. *Clin J Am Soc Nephrol* 2006;1:193–208.
- [12] Rijzewijk LJ, van der Meer RW, Smit JW, Diamant M, Bax JJ, Hammer S, Romijn JA, de Roos A, Lamb HJ. Myocardial steatosis is an independent predictor of diastolic dysfunction in type 2 diabetes mellitus. *J Am Coll Cardiol* 2008;52:1793–9.
- [13] Ng AC, Delgado V, Bertini M, van der Meer RW, Rijzewijk LJ, Shanks M, Nucifora G, Smit JW, Diamant M, Romijn JA, de Roos A, Leung DY, Lamb HJ, Bax JJ. Findings from left ventricular strain and strain rate imaging in asymptomatic patients with type 2 diabetes mellitus. *Am J Cardiol* 2009;104:1398–401.
- [14] Holland DJ, Marwick TH, Haluska BA, Leano R, Hordern MD, Hare JL, Fang ZY, Prins JB, Stanton T. Subclinical LV dysfunction and 10-year outcomes in type 2 diabetes mellitus. *Heart* 2015;101:1061–6.
- [15] Seo Y, Ishizu T, Enomoto Y, Sugimori H, Yamamoto M, Machino T, Kawamura R, Aonuma K. Validation of 3-dimensional speckle tracking imaging to quantify regional myocardial deformation. *Circ Cardiovasc Imaging* 2009;2:451–9.
- [16] Saito K, Okura H, Watanabe N, Hayashida A, Obase K, Imai K, Maehama T, Kawamoto T, Neishi Y, Yoshida K. Comprehensive evaluation of left ventricular strain using speckle tracking echocardiography in normal adults: comparison of three-dimensional and two-dimensional approaches. *J Am Soc Echocardiogr* 2009;22:1025–30.
- [17] Akselrod S, Gordon D, Ubel FA, Shannon DC, Berger AC, Cohen RJ. Power spectrum analysis of heart rate fluctuation: a quantitative probe of beat-to-beat cardiovascular control. *Science* 1981;213:220–2.
- [18] Nakano S, Kitazawa M, Ito T, Hatakeyama H, Nishizawa M, Nakagawa A, Kigoshi T, Uchida K. Insulin resistant state in type 2 diabetes is related to advanced autonomic neuropathy. *Clin Exp Hypertens* 2003;25:155–67.
- [19] Ernande L, Thibault H, Bergerot C, Moulin P, Wen H, Derumeaux G, Croisille P. Systolic myocardial dysfunction in patients with type 2 diabetes mellitus: identification at MR imaging with cine displacement encoding with stimulated echoes. *Radiology* 2012;265:402–9.
- [20] Fang ZY, Yuda S, Anderson V, Short L, Case C, Marwick TH. Echocardiographic detection of early diabetic myocardial disease. *J Am Coll Cardiol* 2003;41:611–617.
- [21] Ernande L, Rietzschel ER, Bergerot C, De Buyzere ML, Schnell F, Groisne L, Ovize M, Croisille P, Moulin P, Gillebert TC, Derumeaux G. Impaired myocardial radial function in asymptomatic patients with type 2 diabetes mellitus: a speckle-tracking imaging study. *J Am Soc Echocardiogr* 2010;23:1266–72.
- [22] Nakai H, Takeuchi M, Nishikage T, Lang RM, Otsuji Y. Subclinical left ventricular dysfunction in asymptomatic diabetic patients assessed by two-dimensional speckle tracking echocardiography: correlation with diabetic duration. *Eur J Echocardiogr* 2009;10:926–32.
- [23] Zhang X, Wei X, Liang Y, Liu M, Li C, Tang H. Differential changes of left ventricular myocardial deformation in diabetic patients with controlled and uncontrolled blood glucose: a three-dimensional speckle-tracking echocardiography-based study. *J Am Soc Echocardiogr* 2013;26:499–506.
- [24] Ishizu T, Seo Y, Kameda Y, Kawamura R, Kimura T, Shimojo N, Xu D, Murakoshi N, Aonuma K. Left ventricular strain and transmural distribution of structural remodeling in hypertensive heart disease. *Hypertension* 2014;63:500–6.
- [25] Chan J, Hanekom L, Wong C, Leano R, Cho GY, Marwick TH. Differentiation of subendocardial and transmural infarction using two-dimensional strain rate imaging to assess short-axis and long-axis myocardial function. *J Am Coll Cardiol* 2006;48:2026–33.
- [26] Poirier P, Bogaty P, Philippon F, Garneau C, Fortin C, Dumesnil JG. Preclinical diabetic cardiomyopathy: relation of left ventricular diastolic dysfunction to cardiac autonomic neuropathy in men with uncomplicated well-controlled type 2 diabetes. *Metabolism* 2003;52:1056–61.
- [27] Sacre JW, Franjic B, Jellis CL, Jenkins C, Coombes JS, Marwick TH. Association of cardiac autonomic neuropathy with subclinical myocardial dysfunction in type 2 diabetes. *JACC Cardiovasc Imaging* 2010;3:1207–15.
- [28] Hage FG, Iskandrian AE. Cardiac autonomic denervation in diabetes mellitus. *Circulation Cardiovasc Imaging* 2011;4:79–81.
- [29] Flotats A, Carrio I. Is cardiac autonomic neuropathy the basis of nonischemic diabetic cardiomyopathy. *JACC Cardiovasc Imaging* 2010;3:1216–8.
- [30] Mochizuki Y, Tanaka H, Matsumoto K, Sano H, Toki H, Shimoura H, Ooka J, Sawa T, Motoji Y, Ryo K, Hirota Y, Ogawa W, Hirata K. Association of peripheral nerve conduction in diabetic neuropathy with subclinical left ventricular systolic dysfunction. *Cardiovasc Diabetol* 2015;14:47.
- [31] Zhen Z, Chen Y, Liu JH, Chan CW, Yuen M, Lam KS, Tse HF, Yiu KH. Increased T-wave alternans is associated with subclinical myocardial structural and functional abnormalities in patients with type 2 diabetes. *J Cardiol* 2016;68:329–34.